Received: 11 April 2018 | Revised: 23 September 2018 | Accepted: 28 September 2018

DOI: 10.1002/bit.26847

ARTICLE

WILEY BIOTECHNOLOGY & BIOENGINEERING

Enhancing hydrogen-dependent growth of and carbon dioxide fixation by *Clostridium ljungdahlii* through nitrate supplementation

David F. Emerson | Benjamin M. Woolston | Nian Liu | Mackenzie Donnelly | Devin H. Currie | Gregory Stephanopoulos

Department of Chemical Engineering, Massachusetts Institute of Technology, Cambridge, Massachusetts

Correspondence
Gregory Stephanopoulos, Department of Chemical Engineering, Massachusetts Institute of Technology, 77 Massachusetts Ave, Cambridge, MA 02139.
Email: gregstep@mit.edu

Funding information
Advanced Research Projects Agency - Energy, Grant/Award Number: DE-AR0000433; U.S. Department of Energy, Grant/Award Number: DE-SC0008744; National Science Foundation, Grant/Award Number: 1122374

Abstract

Synthesis gas (syngas) fermentation via the Wood–Ljungdahl pathway is receiving growing attention as a possible platform for the fixation of CO_2 and renewable production of fuels and chemicals. However, the pathway operates near the thermodynamic limit of life, resulting in minimal adenosine triphosphate (ATP) production and long doubling times. This calls into question the feasibility of producing high-energy compounds at industrially relevant levels. In this study, we investigated the possibility of co-utilizing nitrate as an inexpensive additional electron acceptor to enhance ATP production during H_2-dependent growth of *Clostridium ljungdahlii*, *Moorella thermoacetica*, and *Acetobacterium woodii*. In contrast to other acetogens tested, growth rate and final biomass titer were improved for *C. ljungdahlii* growing on a mixture of H_2 and CO_2 when supplemented with nitrate. Transcriptomic analysis, $^{13}CO_2$ labeling, and an electron balance were used to understand how electron flux was partitioned between CO_2 and nitrate. We further show that, with nitrate supplementation, the ATP/adenosine diphosphate (ADP) ratio and acetyl-CoA pools were increased by fivefold and threefold, respectively, suggesting that this strategy could be useful for the production of ATP-intensive heterologous products from acetyl-CoA. Finally, we propose a pathway for enhanced ATP production from nitrate and use this as a basis to calculate theoretical yields for a variety of products. This study demonstrates a viable strategy for the decoupling of ATP production from carbon dioxide fixation, which will serve to significantly improve the CO_2 fixation rate and the production metrics of other chemicals from CO_2 and H_2 in this host.

KEYWORDS
acetogenic bacteria, anaerobic respiration, *Clostridium ljungdahlii*, fixation, hydrogen, nitrate

1 | INTRODUCTION

Fermentation of synthesis gas (syngas) by autotrophic acetogenic bacteria has received considerable attention as a platform for the renewable production of fuels and chemicals (Hu et al., 2016; Tracy, Jones, Fast, Indurthi & Papoutsakis, 2012). Syngas contains predominantly H_2, CO, and CO_2; when the electrons are derived from H_2, four molecules of H_2 are used to fix two molecules of CO_2 into acetyl-CoA through the Wood-Ljungdahl pathway (WLP). Conversion of acetyl-CoA to acetate provides adenosine triphosphate (ATP) to fuel cellular growth. Some acetogens further convert acetate to ethanol, motivating commercial ventures to produce ethanol from

waste steel mill gas (Ou, Zhang, Zhang & Zhang, 2013). The advent of genetic tools for the model acetogen *Clostridium ljungdahlii* (Köpke et al., 2010) provided an opportunity to divert flux away from acetate to more valuable molecules through metabolic engineering. To date, acetogens have been engineered to produce a variety of chemicals, including butanol (Köpke et al., 2010), butyrate (Ueki, Nevin, Woodard & Lovley, 2014), lactate (Iwasaki et al., 2017), and acetone (Hoffmeister et al., 2016; Jones et al., 2016).

In all reports to date, however, the productivities, titers, and yields have been too low to support a commercially viable process. This is primarily due to energetic considerations. The WLP operates near the thermodynamic limit of life (Schuchmann & Müller, 2014), with a small Gibbs free energy change (Thauer, Jungermann & Decker, 1977):

$$4\ H_2 + 2\ CO_2 \rightleftharpoons CH_3COOH + 2\ H_2O,\ \Delta G_0 = -24\,\text{kJ/mol}\ H_2. \quad (1)$$

Functionally, this means that each mol of acetate produced supports the generation of only 0.25–0.63 mol ATP (Schuchmann & Müller, 2014), leading to low growth yields (0.048 g biomass/g acetic acid; this study) and slow growth rates (t_d > 20 hr on defined medium; Daniel, Hsu, Dean & Drake, 1990). Any diversion of acetyl-CoA flux away from acetate imposes a further ATP penalty on the cell. Simple calculations of the maximal theoretical yield for butanol, for example, suggest an upper limit of 0.2 moles per 100 moles H_2 (Fast & Papoutsakis, 2012).

We hypothesized that cell growth, productivity, and carbon yield in acetogens could, therefore, be improved by providing a cheap, complementary pathway for ATP synthesis. Indeed, recent work in the related acetogen *Clostridium autoethanogenum* showed that arginine supplementation increased growth rate but abolished acetate production during autotrophic growth, by enabling additional ATP production from the conversion of arginine to ornithine (Valgepea, Loi, et al., 2017). However, arginine is an expensive cosubstrate ($9.58 mol^{-1}; 99% FCC FG; Sigma-Aldrich), motivating our search for a cheaper alternative. *C. ljungdahlii* contains a complete set of genes required for nitrate (NO_3^-) assimilation, and heterotrophic growth on fructose with nitrate has been experimentally demonstrated (Nagarajan et al., 2013), but the impact on H_2-dependent CO_2 fixation has not been studied. Since nitrate is a more favorable electron acceptor than CO_2 (Thauer et al., 1977), we reasoned that a controlled redistribution of the electrons from H_2 between CO_2 for carbon fixation and nitrate for ATP synthesis could improve growth:

$$4H_2 + 2H^+ + NO_3^- \rightleftharpoons 3\ H_2O + NH_4^+\ \Delta_r G_0' = -150\,\text{kJ/mol}\ H_2. \quad (2)$$

Previous literature on nitrate metabolism in acetogens paints a confusing picture. In *Moorella thermoacetica* and *Moorella thermoautotrophica*, nitrate has been shown to abolish acetogenesis by the WLP for C1 substrates such as CO, formate, methanol + CO_2, vanillate + CO_2, syringate + CO_2, and H_2 + CO_2 (Fröstl, Seifritz & Drake, 1996; Seifritz, Daniel, Gossner & Drake, 1993). Researchers presumed that nitrate inhibited or blocked the WLP in *M. thermoacetica* (Drake & Daniel, 2004). Growth was only possible in the presence of 1,000 mg/L yeast extract (YE), yet the biomass generated was at most 49 mg/L, hence the fixed carbon was potentially derived from YE. Once YE was removed from the media, growth in the presence of nitrate and a C1 substrate was limited to vanillate+CO and syringate+CO. The impact of nitrate on oxalate and glyoxalate metabolism in *M. thermoacetica* has also been studied (Seifritz, Fröstl, Drake & Daniel, 2002), with similar results. Thus, definitive co-metabolism of nitrate and has not been documented in an acetogen. We set out to test the ability of *C. ljungdahlii* to co-metabolize nitrate and CO_2, additionally employing transcriptomics and metabolomics to examine the regulation of these two processes.

2 | MATERIALS AND METHODS

2.1 | Gases and chemicals

Chemicals were purchased from Sigma-Aldrich (St. Louis, MO). Premixed unlabeled research grade gases were purchased from Airgas (Dorchester, MA). Labeled 99.8% pure $^{13}CO_2$ and $^{15}N_2$ were purchased from Cambridge Isotope Laboratories (Tewksbury, MA). The anaerobic chamber (Coy Laboratories, Grass Lake, MI) atmosphere was 5% H_2, 10% CO_2, and 85% N_2.

2.2 | Bacterial, media, and culture conditions

C. ljungdahlii ATCC 55383 (American Type Culture Collection or ATCC) was grown anaerobically in 125 ml Wheaton serum bottles with butyl rubber stoppers and aluminum crimp seals (Chemglass Life Sciences, Vineland, NJ). Culture volumes of 50 ml were grown at 37°C, pH 6.0, and shaking at 250 rpm with a measured headspace of 107 ml. The headspace was charged to 137.9 kPa (gauge; 20 psig) with 80 mol % H_2 and 20 mol% CO_2, or 80 mol% CO and 20 mol% CO_2. The handling of all live cultures was performed in an anaerobic chamber.

C. ljungdahlii was grown in a medium modified from PETC 1754 (ATCC); in brief, the modifications were: no fructose, 0.1 g/L YE, and 0.3 g/L cysteine. The only available carbon was CO_2, bicarbonate, YE, or cysteine. The modified PETC 1754 medium was prepared by adding 2 g $NaHCO_3$, 1 g NH_4Cl, 0.1 g KH_2PO_4, 0.1 g KCl, 0.2 g $MgSO_4 \cdot 7\ H_2O$, 0.8 g NaCl, 0.02 g $CaCl_2 \cdot 2H_2O$, 0.1 g YE (BD Bacto (TM), BD Biosciences, San Jose, CA) to 970 ml of Milli-Q water. To this 10 ml of vitamin supplement (ATTC), 10 ml of trace mineral supplement (ATTC), and 0.5 ml of resazurin stock solution (0.2% by weight in water) were added. The media was filter sterilized, transferred to the anaerobic chamber, and 10 ml of 3 wt% sterile cysteine stock solution was added. All other media components were prepared anaerobically by sparging with argon for 20 min. Growth was monitored at $OD_{660\,nm}$. For details, see Supporting Information Materials and Methods.

2.3 | Cellular composition

The correlation between $OD_{660\,nm}$ and gDCW/L was determined by harvesting 50 ml of late-exponential phase cells with Whatman

membrane filters (nylon, 0.2 μm pore size, 47 mm diameter) and a vacuum pump. The cells were rinsed twice with 10 ml of millipure water, then dried for 48 hr at 60°C, along with a no-cell control. The elemental composition (C, H, N, S) of biomass and YE was determined with an Elementar Vario EL Cube CHNS. Approximately 5 mg of cell biomass were prepared (in triplicate) and dried by lyophilization. The CHNS was operated under default parameters and standardized with sulfanilamide.

2.4 | Metabolite analytical methods

Formate, acetate, and ethanol were measured by high performance liquid chromatography (HPLC). Nitrate (Cataldo, Maroon, Schrader & Youngs, 1975) and nitrite (Strickland & Parsons, 1972) were measured colorimetrically. Ammonia was measured enzymatically with an Ammonia Assay Kit (Sigma-Aldrich). For details, see Supporting Information Materials and Methods.

2.5 | Derivatization of acetate and formate, and measurement by LC-MS

Acetate and formate were derivatized with a modified procedure from Peters, Hellenbrand, Mengerink and Van Der Wal (2004). Derivatized isotopes were measured by LC/MS/MS with an Agilent (Santa Clara, CA) 1100 separations module equipped with an Agilent Zorbax 300SB-C18 column, and an API 4000 liquid Chromatography with tandem mass spectrometry (LC/MS/MS). For details, see Supporting Information Materials and Methods.

2.6 | RNA isolation, sequencing, and data analysis

When the culture had reached mid-exponential phase, 5 ml of culture was anaerobically collected by centrifugation, and RNA was immediately extracted with an RNeasy Mini Kit (Qiagen, Hilden, Germany), and (gDNA) was removed with DNase (NEB, Ipswich, MA). Samples were sequenced by the BioMicroCenter (MIT, Cambridge, MA). Data were analyzed with Galaxy (https://usegalaxy.org/; Afgan et al., 2016). Raw data were processed with FASTQ Groomer, Bowtie2, and mapped with htseq-count to the EnsemblBacteria genome (http://ensemblgenomes.org/; Kersey et al., 2016). Differential expression was determined with DESeq2 (Dillies et al., 2013; Love, Huber & Anders, 2014). For details, see Supporting Information Materials and Methods.

2.7 | Headspace gas analysis

H_2 was measured with an Agilent Technologies model 7890A gas chromatograph equipped with a thermal conductivity detector and CP-MolSieve 5A capillary column (25 m × 0.320 mm, film thickness 30 μm; Agilent Technologies). CO_2 was measured with an Agilent Technologies model 7890A gas chromatograph equipped with an Agilent Technologies 5975 inert XL mass selective detector and GS-GasPro capillary column (60 m × 0.320 mm; Agilent Technologies). For details, see Supporting Information Materials and Methods.

2.8 | Intracellular metabolite measurement

During the mid-exponential phase, intracellular metabolites were extracted from 3 to 5 ml of culture and quickly transferred to a 0.2 μm nylon membrane within an anaerobic chamber. After filtration, filters were washed with two samples volumes of 4°C water and transferred to a 40:40:20 methanol/acetonitrile/water with 0.1 M formic acid solution on ice in 50-ml Falcon tubes. After 20 min at −20°C, the filters were washed and the metabolite solution was transferred to eppendorf tubes preloaded with 100 μl 15% ammonium bicarbonate. After 10 min of centrifugation at 13,000 rpm and 4°C, the supernatant was dried under nitrogen and resuspended in 40 μl MiliQ water. Metabolite concentrations were quantified with a ultra performance liquid chromatography (UPLC) coupled to a QExactive orbitrap mass spectrometer (Thermo Fisher Scientific, Waltham, MA) with a ZIC-pHILIC (5 μm polymer particle) 150 x 2.1 mm column (MilliporeSigma, Burlington, MA). Total ion counts were processed using MAVEN (Clasquin, Melamud & Rabinowitz, 2012), and natural abundance was corrected with IsoCor (Millard, Letisse, Sokol & Portais, 2012). All measurements were normalized to the control cultures (fructose +CO_2). For details, see Supporting Information Notes on Materials and Methods.

3 | RESULTS AND DISCUSSION

3.1 | *C. ljungdahlii* grows on H_2 and CO_2 with nitrate

To evaluate the potential of nitrate to improve H_2-dependent growth, we inoculated parallel cultures of *C. ljungdahlii*, *Acetobacterium woodii*, and *M. thermoacetica* with a headspace of $H_2 + CO_2$, with or without 15 mM sodium nitrate. In accordance with previous literature (Fröstl et al., 1996), nitrate inhibited acetogenic metabolism of *M. thermoacetica* even though it was growth supportive in the presence of YE (Table 1 and Supporting Information Figure S1). *A. woodii* did not metabolize nitrate Figure 1.

However, the nitrate supplemented $H_2 + CO_2$ *C. ljungdahlii* culture grew robustly, with simultaneous acetate production and stoichiometric conversion of nitrate to ammonium, with little to no production of nitrite (Figure 2a,b). During growth and reduction of nitrate, pH increased from 6.0 to between 7.5 and 8.0. Nitrate-dependent growth continued after several subcultures (Supporting Information Figure S2), confirming that the phenotype was not due to carry-over from the inoculum.

Interestingly, the nitrate-supplemented culture (Figure 2a) significantly outperformed the unsupplemented control (Figure 2c, open symbols), in terms of growth rate (0.084 ± 0.002 vs. 0.048 ± 0.003 hr^{-1}), and final $OD_{660\ nm}$ (0.323 ± 0.001 vs. 0.148 ± 0.011). Moreover, the cellular yield per acetate ($Y_{C/A}$) increased to 0.48 ± 0.03 mol cell carbon per mol acetate with nitrate, from 0.11 ± 0.01 without nitrate (Table 1). Since growth on H_2 + CO_2 is ATP-limited,

TABLE 1 Carbon balance for cultures during the growth phase

	Carbon and Nitrogen balances	ΔBiomass (mM C)	ΔAcetate (mM)	ΔEthanol (mM)	ΔFormate (mM)	Total C (mM C)	ΔNO_3^-(mM)	ΔNO_2^-(mM)	ΔNH_4^+(mM)	ΔBiomass (mM N)	Nitrogen balance
C. ljung	H_2+CO_2 (97 hr)	1.62 (0.13)	15.0 (0.6)	0.6 (0.8)	0.00 (0.00)	32.8 (1.2)					
	H_2+CO_2+NO_3 (42 hr)	4.30 (0.24)	9.02 (0.21)	0.00 (0.07)	5.8 (0.4)	28.1 (0.6)	−11.3 (0.2)	$5 \times 10\ (7 \times 10^{-4})^{-4}$	11.0 (1.5)	1.07 (0.08)	107% (13%)
C. ljung	CO+CO_2 (79 hr)	4.42 (0.19)	19.1 (0.1)	0.63 (0.14)	0.03 (0.04)	42.6 (0.3)					
	CO+CO_2+NO_3 (116 hr)	1.32 (0.18)	1.07 (0.35)	0.39 (0.12)	0.31 (0.07)	3.76 (0.73)	−3.3 (0.8)	3×10^{-2} (1×10^{-2})	6.5 (0.1)	0.33 (0.04)	208% (52%)
M. therm	H_2+CO_2 (96 hr)	1.95 (0.08)	43.0 (0.5)	0.00 (0.00)	0.00 (0.00)	87.9 (1.1)					
	H_2+CO_2+NO_3 (96 hr)	1.49 (0.22)	0.61 (0.21)	0.00 (0.00)	0.00 (0.00)	2.72 (0.33)	−6.6 (0.5)	1.77 (0.05)	1.8 (1.3)	0.37 (0.06)	56% (20%)
A. woodii	H_2+CO_2 (70 hr)	4.23 (0.09)	100.3 (4.5)	0.01 (0.14)	8.3 (0.9)	213 (9)					
YE (0.1 g/L)						3.34 (0.05)				0.80 (0.01)	
Constants		$\frac{gDCW}{L \times OD_{660\,nm}}$	$\frac{gC}{gDCW}$	$\frac{gN}{gDCW}$							
C. ljung	H_2+CO_2	0.377 (0.021)	0.448 (0.015)	0.128 (0.004)							
	H_2+CO_2+NO_3	0.385 (0.016)	0.454 (0.007)	0.132 (0.002)							
YE			0.401 (0.006)	0.113 (0.002)							

Note. Values were determined by subtracting the initial time point from the concentration at peak OD; this time is indicated under the substrate. Negative values imply consumption. The nitrogen balance was calculated by dividing the nitrogenous products by the nitrate consumed. Constants used to calculate mM C of biomass from optical density, as well as the total C and N contribution from YE. YE total C are provided. The total carbon and nitrogen that could be derived from yeast extract (YE) are given in the bottom "YE" row. The dry cell weight correlation ($gDCW \cdot L^{-1} \cdot OD^{-1}$) was determined experimentally for *C. ljungdahlii*, and taken from the literature for *M. thermoacetica* (Sakai et al., 2005), and *A. woodii* (Demler & Weuster-Botz, 2011). Standard deviation is given in parentheses for three biological replicates.

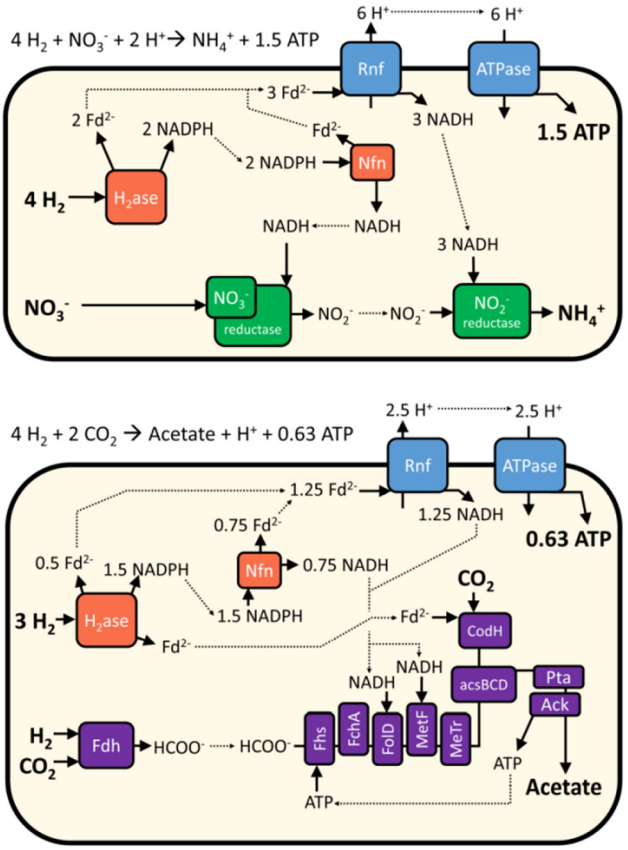

FIGURE 1 Enzymes and reducing equivalents necessary for H_2 energy conservation and ATP production in *C. ljungdahlii* with nitrate (top) or CO_2 (bottom) as the reducing equivalent. Nitrate is proposed as an electron sink for reducing equivalents from the Rnf complex but is not directly involved in ATP generation. The stoichiometries for proton translocation and ATP synthase were derived from Schuchmann and Müller (2014). Rnf: Rhodobacter nitrogen fixation [Color figure can be viewed at wileyonlinelibrary.com]

the increased $Y_{C/A}$ implies that additional ATP was generated from nitrate reduction. Despite the increased growth rate, nitrate supplementation led to a decrease in the WLP-cell-specific productivity (0.28 ± 0.02 vs. 0.45 ± 0.02 mmol $C \cdot hr^{-1} \cdot L^{-1}$). However, due to the higher growth rate and optical density, volumetric productivity was increased (0.47 ± 0.01 vs. 0.38 ± 0.02 mmol $C \cdot hr^{-1} \cdot L^{-1}$; Supporting Information Figure S3).

After 52 hr, nitrate was depleted, leading to a halt in acetate secretion and a significant drop in optical density. We presume that this death phase was caused by a metabolism crash; after nitrate was depleted, the WLP was not sufficient to supply the ATP necessary for growth and maintenance of such a dense culture (Valgepea, de Souza Pinto Lemgruber, et al., 2017). After another approximately 60 hr, acetate secretion resumed in unison with the onset of formate consumption. This metabolism was likely dependent on the metabolism of the remaining H_2 + CO_2 and formate by metabolically active cells resulting in growth. As nitrate was long depleted from the medium, this acetate production was likely unrelated to the earlier presence of nitrate.

Considering the advantage nitrate provided to growth on H_2, we wondered if the same growth benefits would be observed in the presence of CO as the electron source. Indeed, when CO was the sole electron source and nitrate was supplemented, *C. ljungdahlii* grew slower, and to a lower $OD_{660\,nm}$ (Figure 3). During this time, only 1.07 ± 0.35 mM acetate and 0.39 ± 0.12 mM ethanol were produced, see Table 1. Instead, nitrate was reduced, and ammonium was produced. In stark contrast with H_2 cultures, there was substantial nitrite production within the first 45 hr with a high of 163 μM and an average of 131 ± 40 μM. From metabolite balances alone, the cause for slow growth was unclear.

Interestingly, when *C. ljungdahlii* was grown on CO + CO_2 + NO_3^-, more ammonia was generated that could be derived from nitrate. At first, we considered if the slow growth and excess ammonia could be explained by N_2 fixation, as *C. ljungdahlii* has been shown to fix N_2 (Tremblay, Zhang, Dar, Leang & Lovley, 2013), and N_2 fixation would be ATP intensive. The N_2 source was the atmosphere of the anaerobic chamber and it was present within the serum bottles at approximately 100 kPa (gauge). To determine if N_2 fixation occurred, *C. ljungdahlii* was grown in media lacking NH_4^+. The medium was prepared in the serum bottle, degassed with a vacuum pump, and was provided either labeled or unlabeled N_2. Labeled or unlabeled nitrate was provided as indicated. Labeled ammonium was only observed when labeled nitrate was provided. But there was a substantial fraction that was unlabeled and was not derived from either $^{15}N_2$ or $^{15}NO_3^-$ (Figure 4). No labeling was observed in the absence of labeled nitrate. Presumably, a significant portion of this unaccounted nitrogen could be derived from YE (0.8 mM N; Table 1). The rest was likely derived from cysteine, the only other nitrogen source in the medium.

As N_2 fixation did not occur, there was no explicit reason for the observed phenotype (slow growth and low titers). Regardless, these were important findings, as further research in this direction could elucidate how acetogens regulate metabolism on various electron donors and acceptors. In particular, the stark contrast between growth on H_2 + NO_3^- and CO + NO_3^- could help unravel the intricacies of autotrophic growth in the presence of nitrate; this study is ongoing. Despite the interesting but conflicting results, the rest of this study will focus on H_2 and nitrate metabolism by *C. ljungdahlii*.

3.2 | Mass balances and $^{13}CO_2$ labeling confirm CO_2 fixation

While previous reports indicated that *M. thermoacetica* required YE for growth on H_2 + CO_2 + NO_3^- (Fröstl et al., 1996), YE was not fundamentally necessary for the growth of *C. ljungdahlii* with H_2 + CO_2 + NO_3^- (Supporting Information Figure S4). Instead, YE was necessary for robust growth on H_2 + CO_2. The 0.1 g/L would, at most, contribute 3.34 ± 0.05 mM C to the 27.6 ± 0.6 mM C fixed (Table 1); however, the YE could contribute substantially to biomass, which reached only 4.30 ± 0.24 mM C.

To further verify that CO_2 was reduced and fixed to acetate by *C. ljungdahlii*, $^{13}CO_2$ was provided to the headspace in place of CO_2. Both cultures ($^{13}CO_2$ + H_2 and $^{13}CO_2$ + H_2 + NO_3^-) exhibited significant labeling of acetate as M + 1 and M + 2 (Figure 5a). This validates

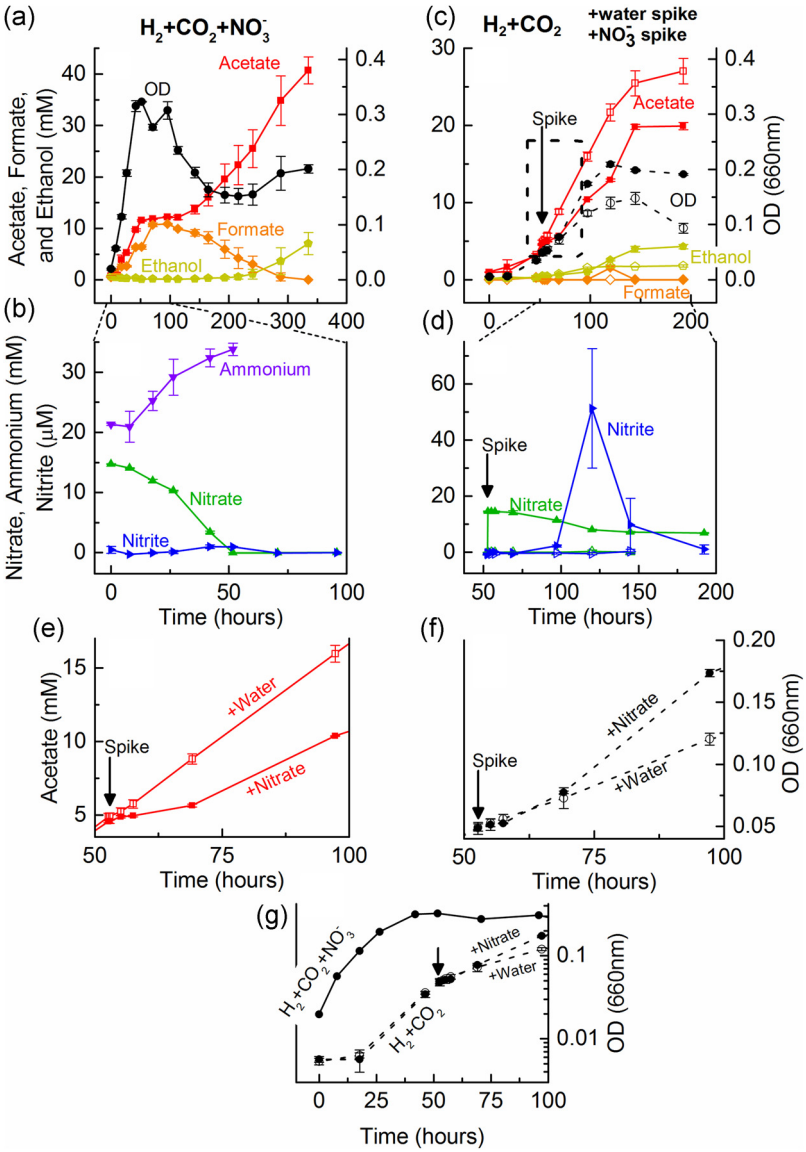

FIGURE 2 Metabolite concentrations and optical density of *C. ljungdahlii* with H_2 and CO_2 as the electron and carbon source. Cultures either contained nitrate (a,b) or received a spike of nitrate (closed symbols) or water (open symbols) at 52 hr (c). RNA was extracted 5 min before and 2 hr after this spike. Acetate (e) and $OD_{660\,nm}$ (f) are given for 50 hr after the spike. (g) Growth curves from panels (a) and (b) are presented in a semi-log plot. Black circle: $OD_{660\,nm}$; red square: acetate; orange diamond: formate; yellow pentagon: ethanol; green up-arrow: nitrate; blue right-arrow: nitrite; purple down-arrow: ammonium. Metabolite units are in mM, except nitrite which is in μM. Standard deviations are given for three biological replicates [Color figure can be viewed at wileyonlinelibrary.com]

that CO_2 was indeed fixed in the presence of nitrate, and suggests that the nitrate inhibitory mechanisms predicted in *M. thermoacetica* (Drake & Daniel, 2004) was not operating in *C. ljungdahlii*; the large M + 2 fraction indicated that neither branch of the WLP was blocked. Unlabeled carbons could be attributed to either the unlabeled bicarbonate (present in all cultures), YE, or the inoculum, as represented experimentally by replacing $^{13}CO_2$ with N_2 ($N_2 + H_2 + NO_3^-$). The effect of the inoculum was accounted for by removing H_2 from the headspace ($N_2 + NO_3^-$), and resulted in little to no growth as compared with when H_2 and nitrate were present (Figure 5b).

To ensure that only H_2 and nitrate were responsible for the increase in growth yield, a detailed H_2 balance was performed by comparing changes in headspace pressure and metabolite concentrations for cultures (see Supporting Information Figure S2). The measured values of H_2 consumption matched closely with those determined theoretically, and the balance was close to 80 ± 4% for the $H_2 + CO_2$ cultures, and 101 ± 1% for $H_2 + CO_2 + NO_3^-$ cultures (Figure 5c; Supporting Information Table SII). This indicated that almost all electron donors and acceptors were accounted for in these experiments; for the $H_2 + CO_2$ culture, the discrepancy of excess reducing equivalents could be attributed to YE, as designated by the dashed line in Figure 5c. This implies that nitrate reduction was directly responsible for the increase in growth yield.

3.3 | A proposed model for nitrate-dependent ATP production in *C. ljungdahlii*

That nitrate reduction was coupled to ATP production was surprising because nitrate reduction in *C. ljungdahlii* was predicted to be assimilatory. Typically assimilatory nitrate reduction is not energy conserving as it occurs in the cytoplasm (Moreno-Vivián, 1999). The other two known nitrate reduction systems, respiratory and fermentative, are energy-conserving (Hasan & Hall, 1975; Moreno-Vivián, 1999). Respiratory nitrate reduction involves a Q loop to couple nitrate

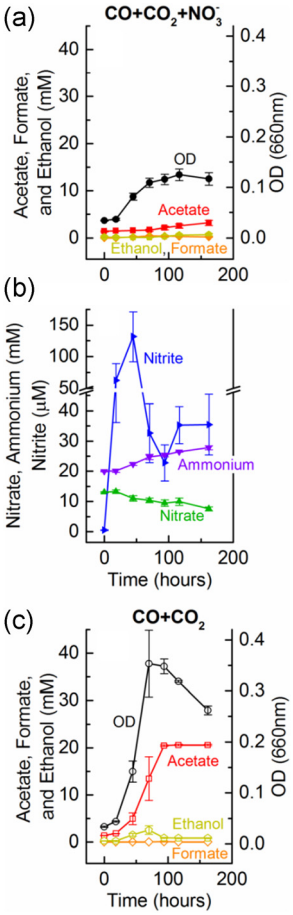

FIGURE 3 Metabolite concentrations and optical density of *C. ljungdahlii* with CO and CO_2 as the electron and carbon source, with (a,b; closed symbols) and without (c; open symbols) nitrate. Black circle: $OD_{660\,nm}$; red square: acetate; orange diamond: formate; yellow pentagon: ethanol; green up-arrow: nitrate; blue right-arrow: nitrite; purple down-arrow: ammonium. Metabolite units are in mM, except nitrite which is in μM. Standard deviations are given for three biological replicates [Color figure can be viewed at wileyonlinelibrary.com]

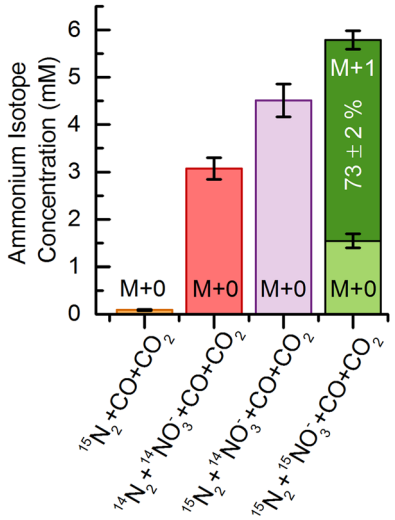

FIGURE 4 The absence of labeling in ammonium from $^{15}N_2$ demonstrates the absence of N_2 fixation. *C. ljungdahlii* was grown in medium lacking NH_4^+, and was provided 100 kPa (gauge) of either labeled or unlabeled N_2. Where indicated, labeled or unlabeled nitrate was added at a concentration of 15 mM. M + 0 indicates unlabeled and M + 1 indicates labeled ammonium. Standard deviations are given for biological triplicates. Values corrected for natural abundance [Color figure can be viewed at wileyonlinelibrary.com]

reduction to ATP generation (Jormakka, Byrne & Iwata, 2003). Fermentative nitrate reduction redirects carbon flow to pathways with substrate level phosphorylation (Hasan & Hall, 1975). *M. thermoacetica* was predicted to respire nitrate, as its genome contains genes similar to *E. coli's* membrane-bound nitrate reductase (Pierce et al., 2008) and has the genes necessary to synthesize cytochromes and quinones. *C. ljungdahlii*, on the other hand, does not contain the genes necessary for cytochrome or quinone synthesis (Köpke et al., 2010) and, thus, is not predicted to respire nitrate. Furthermore, energy conservation by fermentative nitrate reduction was inconsistent with our experimental results (Table 1).

During autotrophic growth, energy conservation in *C. ljungdahlii* is mediated by the Rhodobacter nitrogen fixation (Rnf) complex, which catalyzes the highly exergonic transfer of electrons from reduced ferredoxin to NAD^+, using the free energy released to translocate protons across the cell membrane. These protons are then imported through an ATPase, leading to the production of ATP. It, therefore, seemed likely that the Rnf complex played a role in ATP generation from nitrate reduction. Figure 1 shows a hypothetical pathway for the Rnf-dependent generation of ATP from nitrate reduction. In this pathway, four molecules of H_2 are oxidized, reducing $2NADP^+$ and 2 ferredoxin (Fd; Mock et al., 2015). The 2NADPH are converted into NADH and reduced ferredoxin (Fd^{2-}). The $3Fd^{2-}$ are reoxidized at the Rnf complex, leading to the formation of 3NADH, and the extrusion of $6H^+$. The $6H^+$ are reimported through the ATPase, generating 1.5 molecules of ATP. Meanwhile, the 4NADH are reoxidized in the cytosolic reduction of nitrate to ammonium. The net stoichiometry is (Thauer et al., 1977):

$$4\,H_2 + 2\,H^+ + NO_3^- + 1.5\,ADP + 1.5\,P_i \rightleftharpoons 4\,H_2O + NH_4^+ + 1.5\,ATP \quad \Delta_r G_0' = -138\ kJ\ mol^{-1}.H_2 \tag{3}$$

The proposed mechanism relies on electron bifurcation by the hydrogenase to couple nitrate reduction to ATP production without the need for a membrane-bound nitrate reductase. Though this mechanism is hypothetical, there is precedent from caffeate reduction in *A. woodii*, which produces 1 mol of ATP per mol of caffeate by a similar Rnf-dependent mechanism (Biegel & Muller, 2010; Imkamp, Biegel, Jayamani, Buckel & Müller, 2007; Tschech & Pfennig, 1984).

Importantly, the proposed mechanism is completely independent of carbon metabolism and provides more ATP than the production of acetate from H_2 (1.5 vs. 0.63) by allowing Fd^{2-} oxidation to be coupled to energy conservation, rather than to CO_2 reduction to CO. These theoretical predictions were broadly consistent with our experimental data averaged during the growth phase, where 0.296 ± 0.005 mol ATP per mol acetate was produced by the WLP and 0.801 ± 0.023 mol ATP

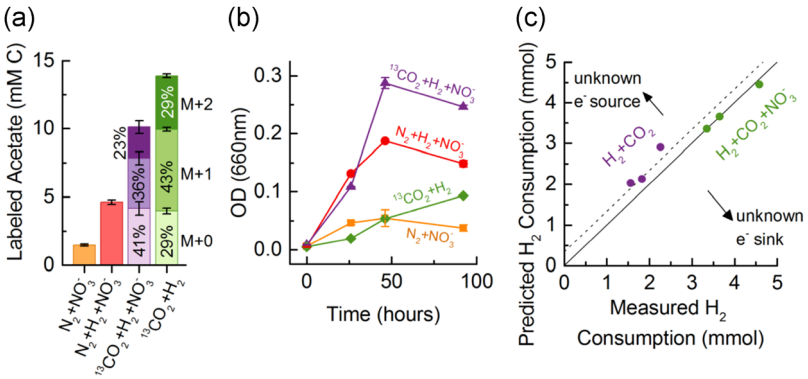

FIGURE 5 Labeling of acetate from $^{13}CO_2$ verified CO_2 fixation and the H_2 balance confirmed that H_2 and nitrate were responsible for improved growth rates and yields. (a) *C. ljungdahlii* was grown in medium containing bicarbonate, with or without nitrate, and various gases in the headspace. When a gas was excluded, N_2 was supplemented at the same partial pressure. The labeling pattern of acetate is given at the final time point as a percentage and corrected for natural abundance. The unlabeled carbon was likely derived from bicarbonate based on the $^{13}CO_2$ control (N_2 + H_2 + NO_3^-. M + 1 corresponds to one ^{13}C, and M+2 corresponds to two ^{13}C incorporated into acetate. (b) Growth curves during labeling experiment. (c) Measured H_2 consumption was compared with predicted H_2 consumption; the prediction was based on the reduction of CO_2 to acetate, formate, and cells or nitrate to ammonium and cells. The possible contribution of YE is accounted for with the dashed line. (a,b) Standard deviations are given for biological duplicates. (c) Each point is a single culture. YE: yeast extract [Color figure can be viewed at wileyonlinelibrary.com]

per mol of nitrate by nitrate reduction (see Supporting Information Notes on Cellular and ATP Yields Calculations).

3.4 | Nitrate increases ATP/ADP ratio and acetyl-CoA pool size when the electron source was H_2

To further investigate the increase in ATP production from nitrate metabolism, intracellular metabolites were measured at mid-exponential phase for *C. ljungdahlii* grown on fructose + CO_2, H_2 + CO_2, or CO + CO_2, with and without nitrate. Of significant importance were the ATP/ADP ratio and the acetyl-CoA pool size (Figure 6) because the former informs on the energetic state of the cell, and the size of the acetyl-CoA pool has been linked to metabolic collapse in energetically limited cells (Valgepea, de Souza Pinto Lemgruber, et al., 2017). The ATP/ADP ratio increased in the presence of nitrate when the electron source was fructose or H_2. For the H_2 + CO_2 culture, this was a 5.3 ± 0.9-fold increase, and the ATP/ADP ratio approached that of the fructose culture. The acetyl-CoA pool size only increased in the presence of nitrate when the substrate was H_2 + CO_2, again to levels comparable to the fructose-grown culture (a 2.8 ± 0.9-fold increase). Taken together, these data suggest that nitrate significantly enhances the energetic state of the cell during growth on H_2, by increasing the supply of both acetyl-CoA and ATP.

Conversely, when *C. ljungdahlii* was grown on CO + CO_2 + NO_3^-, the ATP/ADP ratio fell 2.7 ± 1.5-fold, as compared with growth on CO + CO_2. Moreover, the acetyl-CoA pool size dropped by 2.8 ± 0.9-fold. The decrease in ATP/ADP ratio and acetyl-CoA pool size either explained or was symptomatic of the poor growth on CO + CO_2 + NO_3^- (Figure 3).

Other intracellular metabolites were measured, including from gluconeogenesis and different amino acid biosynthesis pathways. Of note, during growth on H_2, the presence of nitrate generally increased metabolite pool sizes of those in gluconeogenesis, except pyruvate. The opposite was true during growth on CO. Unlike the metabolites of gluconeogenesis, the various measured amino acids generally decreased in concentration when the substrate was H_2 + CO_2 + NO_3^- versus H_2 + CO_2. The most apparent was lysine, which decreased by 5.1 ± 1.4-fold. This concentration was 30 ± 4-fold less than that observed in the fructose grown culture. Of the measured amino acids, only arginine and glutamate increased in concentration, though the increase was moderate (2.2 ± 1.4- and 1.4 ± 0.2-fold, respectively). This depletion could be explained by a higher growth rate requiring the amino acids for protein synthesis. In future fermentations, supplementation of these key metabolites to the media may have marked improvements on the growth rate and titer, especially lysine, which was essentially depleted.

The most striking change was that of α-ketoglutaric acid (αKG) when grown on CO + CO_2 + NO_3^-. Intracellular concentrations for αKG when grown on CO + CO_2 were already comparable to that when grown on fructose. When nitrate was added, there was a 4.7 ± 2.1-fold increase in concentration. α KG is part of the branched

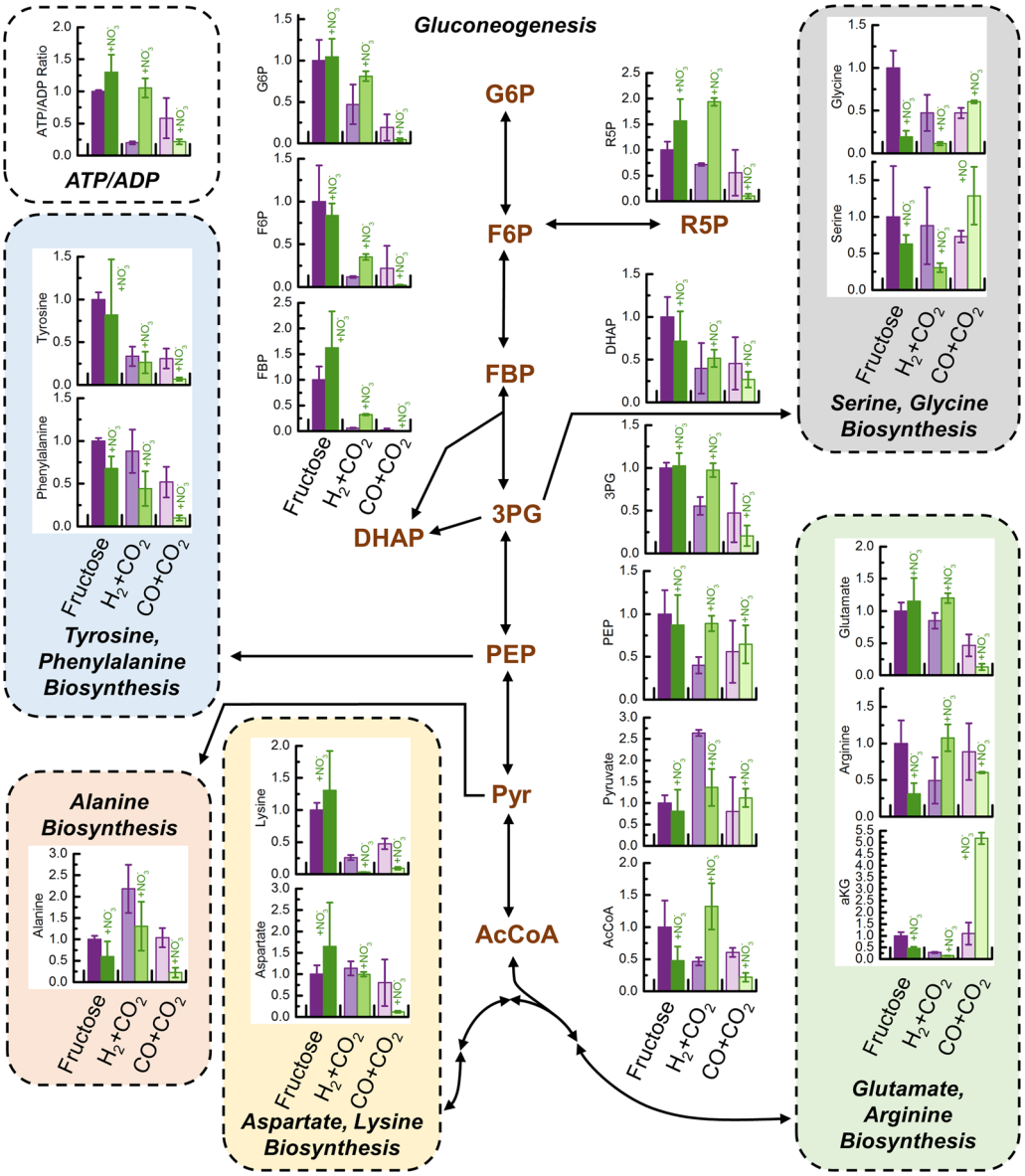

FIGURE 6 Normalized intracellular metabolites of *C. ljungdahlii* were measured during mid-exponential phase while grown on fructose + CO_2, H_2 + CO_2, or CO + CO_2, with and without nitrate. Metabolite pool sizes were normalized to fructose grown cultures. Standard deviation is given in parentheses for three biological replicates. AcCoA: acetyl-CoA; DHAP: dihydroxyacetone phosphate; FBP: fructose 1,6-bisphosphatase; F6P: fructose 6-phosphate; G6P: glucose 6-phosphate; PEP: phosphoenolpyruvic acid; Pyr: pyruvate; R5P: ribose 5-phosphate; 3PG: 3-phosphoglyceric acid [Color figure can be viewed at wileyonlinelibrary.com]

TCA cycle present in *C. ljungdahlii* (Köpke et al., 2010; Tan, Liu, Chen, Zheng & Li, 2013). Thus, this result could not be explained by cellular metabolism of cysteine, a media component, and the predicted source of excess ammonium. Instead, accumulation could result from the stresses placed onto the cell or the cells attempt to regulate metabolism (Doucette, Schwab, Wingreen & Rabinowitz, 2011).

3.5 | RNA transcriptome response of *C. ljungdahlii* to nitrate

We next used transcriptomics to analyze global gene expression in *C. ljungdahlii* during growth on H_2 + CO_2, with or without nitrate. Samples were taken at multiple time points, in an effort to better understand how electron flux was partitioned between nitrate and CO_2. To probe expression profiles, cultures were grown with or without nitrate, and RNA samples were taken during mid-exponential phase (Figure 2g), the $\log_2$ fold change was quantified between the nitrate and the no-nitrate samples. For the dynamic transcriptome change, cultures were grown without nitrate. At approximately 1/3 the final expected OD (0.05 $OD_{660\,nm}$), an RNA sample was extracted. Five minutes later, the cultures received either a nitrate spike or water control spike (Figure 2c). RNA was then extracted 2 hr after, and the $\log_2$ fold change was quantified between the two time points for a given culture. The $\log_2$ fold change in expression for the

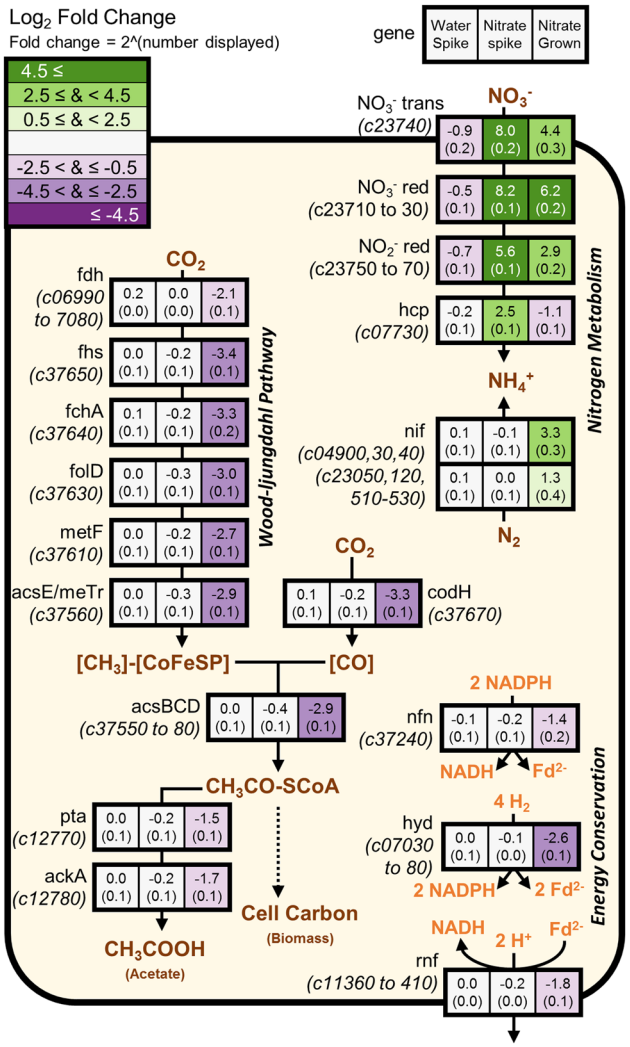

FIGURE 7 Log_2 fold change in expression for RNA transcripts in *C. ljungdahlii* related to the WLP, nitrogen, or energy metabolism. The left-most and middle box is the change after receiving a water and nitrate spike, respectively. The right-most box is the fold increase of cultures grown on nitrate versus those grown without. The fold change of spiked cultures compares 2 hr after versus 5 min before the spike. Green indicates an increase in transcript levels in the presence of nitrate, whereas purple indicates a decrease. For enzymes with subunits, an average is given. Standard deviations are is given in parentheses for three biological replicates.
WLP: Wood–Ljungdahl pathway [Color figure can be viewed at wileyonlinelibrary.com]

WLP genes and putative nitrate reduction pathway genes for each condition is shown in Figure 7.

Within 2 hr of receiving the nitrate spike, transcripts related to nitrate metabolism rose dramatically (Figure 7, middle boxes; e.g., 8.2 log_2 fold for the nitrate reductase, NO_3^- red). Curiously, levels of WLP transcripts were unchanged during this time. When grown on nitrate (Figure 7, right boxes), genes involved in nitrate metabolism were highly upregulated compared with the no-nitrate control (e.g., 6.2 log_2 fold for the nitrate reductase). By contrast, genes involved in the WLP were significantly downregulated (e.g., 2.9 log_2 fold for the acetyl-CoA synthase, acsBCD), which was consistent with the lower specific flux through the WLP discussed earlier.

After receiving the nitrate spike (Figure 2e,f), growth and acetate production did not substantially change within 2 hr, similar to the WLP transcripts. After 5 hr, acetate production slightly diverges; only after 15 hr was this divergence substantial. Growth only diverged after 44 hr.

Comparing the time-dependent change in transcripts and metabolism after the addition of nitrate provides clues to the mechanism involved. Within 2 hr there was no change in WLP transcripts in response to nitrate, hence nitrate likely did not directly repress WLP transcription with a sensor/regulator; this time frame would be sufficient time for significant RNA transcript turnover if WLP transcripts were tightly repressed (Esquerré et al., 2015; Pedersen, Reeh & Friesen, 1978; Supporting Information Figure S5). Conversely, the rapid upregulation of the nitrate reduction system suggests control by a sensor/regulator system. Because acetate production only slightly diverged after 5 hr, enzyme inhibition or competition was likely not a key mediator even though some formate dehydrogenases are inhibited by nitrate (Allais, Louktibi & Baratti, 1983; Blanchard & Cleland, 1980; Schüte, Flossdorf, Sahm & Kula, 1976; Schauer & Ferry, 1982). Instead, the substantial divergence of acetate production at 15 hr corresponded closely to WLP transcript downregulation (Figure 7, right boxes) and the time frame of bacterial protein turnover (~20 hr; Maier et al., 2011; Moran et al., 2013). One possibility was that changes in the cellular redox environment caused this shift in metabolism when nitrate was introduced (Kracke, Virdis, Bernhardt, Rabaey & Krömer, 2016). Other mechanisms were also possible. Further experimentation will be required to fully understand how electron flux is partitioned between CO_2 and nitrate.

3.6 | Nitrate assimilation improves the theoretical yield of acetyl-CoA-derived products

ATP limitation is the leading hypothesized cause of the low yields for the production of heterologous chemicals through syngas fermentation (Fast & Papoutsakis, 2012; Molitor, Marcellin & Angenent, 2017). We, therefore, asked whether supplementation of nitrate to boost ATP production could lead to higher yields of these products, by reducing the amount of acetyl-CoA that must be converted to acetate for ATP production. While this intrinsically diverts electrons from product synthesis, we theorized that more efficient ATP production would still improve titers and yields. To probe this question, we calculated the theoretical yield of various chemicals (Bertsch & Müller, 2015) produced from H_2 + CO_2, with and without nitrate, using the experimentally determined ATP yields (see Supporting Information Notes on Cellular and ATP Yields Calculations). The yields are shown in Table 2 and the stoichiometries in Table 3.

For every product examined, both the hydrogen yield (Y_H) and the carbon yield (Y_c) improved significantly with the supplementation of nitrate. The greatest benefit was realized in pathways where significant amounts of additional ATP were required for product biosynthesis. For

TABLE 2 Carbon and H_2 yield, and lab scale cost for producing chemicals from $H_2 + CO_2$ with and without nitrate

	$H_2 + CO_2$			$H_2 + CO_2$ + nitrate		
Products (#C)	$ mol/C	Y_{H2}%	Y_C%	$ mol/C	Y_{H2}%	Y_C%
Biomass (1)	29.09	6	5	9.01	14	100
Acetate (2)	1.57	94	95	—	—	—
Ethanol (2)	5.05 1.93	41 94	31 93	2.74 —	64 —	95 —
S-3HB (4)	6.13	27	24	2.86	49	95
R-3HB (4)	3.91	41	39	2.25	65	95
Isoprene (5)	12.80	16	14	4.79	34	96
Lactate (3)	4.91 3.58	30 36	22 27	2.47 2.25	53 59	93 93
2,3-Butanediol (4)	6.59	29	23	3.10	53	95
Acetone (3)	4.54	41	41	2.53	64	96
Isobutene (4)	8.60	25	25	3.70	47	97

Note. A basis of 1 mol of the product was chosen, and the number of C in the product is given. Depending on the condition, acetate was produced or nitrate consumed to generate the necessary ATP. Y_c represents the theoretical maximum carbon yield, as determined by the carbon present in the product divided by the carbon dioxide consumed. Y_{H2} represents the H_2 electrons present in the product per total consumed. The cost of the substrate per mole of carbons in the product is given ($mol/C). The cost basis was $0.86 per mol nitric acid (6× 2.5 L; Sigma), $0.33 per mol H_2 (260 std ft^3, Ultrahigh purity; Airgas), and $0.82 per mol CO_2 (260 std ft^3, Research grade; Airgas). If CO_2 can be acquired at no cost, production with nitrate remains cheaper than without for all products.

instance, when producing isoprene from H_2+CO_2 alone, Y_c was only 14%; the rest was diverted to acetate for ATP. When nitrate was present, however, acetate production was not theoretically necessary for ATP generation and Y_c was 96%, a 6.9-fold increase of the theoretical Y_c. These yields increased because, theoretically, no acetate must be produced for ATP production, and ATP production by nitrate reduction was more efficient on the basis of H_2. Furthermore, adding nitrate (as nitric acid) decreased the calculated cost per mole of product, due to lowering the H_2 and CO_2 requirement per mole of product (as determined from lab scale quantities). For these reasons, nitrate supplementation could greatly improve CO_2 fixation and chemical production with H_2. However, controlling electron flux between nitrate and CO_2, and ensuring high expression of the WLP are key considerations in future research.

4 | CONCLUSION

Unlike other studied acetogens, *C. ljungdahlii* was able to simultaneously reduce CO_2 and nitrate, with electrons derived from H_2. Cultures supplemented with nitrate grew faster, and to higher optical densities, than those without, as verified via carbon and H_2 balances, and ^{13}C labeling. We further showed that nitrate reduction was coupled to ATP generation, which was corroborated by a fivefold increase of the ATP/ADP ratio. We proposed a mechanism for the energetic coupling. The 40% decrease in cell-specific WLP activity could be explained with transcript downregulation of the associated enzymes, but the transcriptional regulation was not direct. The ability to decouple ATP production from the WLP during growth on H_2 + CO_2 has important implications for improving the selectivity of products produced with this organism, as well as redirecting carbon flux from acetate to desirable product, as shown by theoretical calculations. To take full advantage of this novel metabolic capability, future work will be directed at elucidating and controlling of electron flow between nitrate and CO_2. This discovery has significant implications for current industrial autotrophic fermentations when the product is not ethanol or acetate.

TABLE 3 Theoretical carbon, hydrogen, and nitrate balance for producing chemicals from H_2 + CO_2 with and without nitrate

			H_2+CO_2			H_2+CO_2+nitrate		
Products (#C)	Pathway	Substrates Bio	CO_2	H_2	Acetate	CO_2	H_2	Nitrate
Biomass (1)		1.00	−19.59	−39.48	9.29	−1.00	−15.93	−3.41
Acetate (2)	Acetate kinase	0.11	−2.11	−4.25	1	—	—	—
Ethanol (2)	Acetaldehyde DH AOR	0.10 0.15	−6.37 −2.15	−14.76 −6.35	2.13 0	−2.1 —	−9.36 —	−0.78 —
S-3HB (4)		0.20	−16.33	−33.73	6.07	−4.2	−18.36	−2.23
R-3HB (4)		0.20	−10.33	−21.71	3.06	−4.2	−13.95	−1.12
Isoprene (5)	Mevalonate	0.25	−42.35	−88.77	18.55	−5.25	−41.79	−6.8
Lactate (3)	NADH dependent Bifurcating LDH	0.15 0.15	−9.95 −6.35	−19.94 −16.74	3.4 2.6	−3.15 −3.15	−11.33 −10.16	−1.25 −0.95
2,3-Butanediol (4)	Acetolactate	0.20	−17.13	−37.33	6.47	−4.2	−20.95	−2.37
Acetone (3)	Acetoacetate	0.15	−8.75	−19.54	2.8	−3.15	−12.45	−1.03
Isobutene (4)	Acetone, 3-OH-isovalerate	0.20	−22.34	−48.75	9.07	−4.2	−25.77	−3.33

Note. Products were listed with the number of carbons in the molecule along with the pathway of production. A basis of 1-mole product was assumed, with the production/consumption of all other products/ reactants participating in the balances reported in moles. Biomass production was set at 5% of the carbons in the product.

AUTHOR CONTRIBUTIONS

D. F. E., B. M. W., D. C., and G. S. designed the research; D. F. E., N. L., and M. D. performed the research; D. F. E. and N. L. analyzed data; and D. F. E., B. M. W., D. C., and G. S. wrote the manuscript. All authors read and approved the final manuscript.

ACKNOWLEDGMENTS

We are grateful to Dan Hoer of the Girguis Lab at Harvard for headspace gas analysis of H_2 and CO_2. D. F. E., B. M. W., and D. H. C. are supported by the Advanced Research Projects Agency Energy under the Award DE-AR0000433. B. M. W. is additionally supported by the National Science Foundation Graduate Research Fellowship under Grant No. 1122374. N. L. is supported by the U.S. Department of Energy Genomic Science research program under Grant number DE-SC0008744.

CONFLICTS OF INTEREST

The authors declare no conflicts of interest.

DATA AVAILABILITY

The data reported in this paper will be deposited in the Gene Expression Omnibus (GEO) database upon acceptance, www.ncbi.nlm.nih.gov/geo.

ORCID

David F. Emerson http://orcid.org/0000-0003-4948-9962
Benjamin M. Woolston http://orcid.org/0000-0002-6570-2236

REFERENCES

Afgan, E., Baker, D., van den Beek, M., Blankenberg, D., Bouvier, D., Čech, M., & Goecks, J. (2016). The Galaxy platform for accessible, reproducible and collaborative biomedical analyses: 2016 update. *Nucleic Acids Research.*, *44*, W3–W10.

Allais, J. J., Louktibi, A., & Baratti, J. (1983). Oxidation of methanol by the yeast Pichia pastoris. Purification and properties of the formate dehydrogenase. *Agricultural and Biological Chemistry*, *47*, 2547–2554.

Bertsch, J., & Müller, V. (2015). Bioenergetic constraints for conversion of syngas to biofuels in acetogenic bacteria. *Biotechnology Biofuels*, *8* (1), 210.

Biegel, E., & Muller, V. (2010). Bacterial Na+-translocating ferredoxin: NAD+ oxidoreductase. *Proceedings of the National Academy of Sciences of the United States of America*, *107*(42), 18138–18142.

Blanchard, J. S., & Cleland, W. W. (1980). Kinetic and chemical mechanisms of yeast formate dehydrogenase. *Biochemistry*, *19*(15), 3543–3550.

Cataldo, D., Maroon, M., Schrader, L., & Youngs, V. (1975). Rapid colorimetric determination of nitrate in plant tissue by nitration of salicylic acid. *Communications in Soil Science and Plant Analysis*, *6*(1), 71–80.

Clasquin, M. F., Melamud, E., & Rabinowitz, J. D. (2012). LC-MS data processing with MAVEN: A metabolomic analysis and visualization engine. *Current Protocols in Bioinformatics*, *14*(37), 11.1–14.11.

Daniel, S. L., Hsu, T., Dean, S. I., & Drake, H. L. (1990). Characterization of the H2- and CO-dependent chemolithotrophic potentials of the acetogens Clostridium thermoaceticum and Acetogenium kivui. *Journal of Bacteriology*, *172*(8), 4464–4471.

Demler, M., & Weuster-Botz, D. (2011). Reaction engineering analysis of hydrogenotrophic production of acetic acid by Acetobacterium woodii. *Biotechnology and Bioengineering*, *108*(2), 470–474.

Dillies, M. A., Rau, A., Aubert, J., Hennequet-Antier, C., Jeanmougin, M., Servant, N., & Jaffrézic, F. (2013). A comprehensive evaluation of normalization methods for Illumina high-throughput RNA sequencing data analysis. *Briefings in Bioinformatics*, *14*(6), 671–683.

Doucette, C. D., Schwab, D. J., Wingreen, N. S., & Rabinowitz, J. D. (2011). A-ketoglutarate coordinates carbon and nitrogen utilization via enzyme I inhibition. *Nature Chemical Biology*, *7*(12), 894–901.

Drake, H. L., & Daniel, S. L. (2004). Physiology of the thermophilic acetogen Moorella thermoacetica. *Research in Microbiology*, *155*(10), 869–83.

Esquerré, T., Moisan, A., Chiapello, H., Arike, L., Vilu, R., Gaspin, C., & Girbal, L. (2015). Genome-wide investigation of mRNA lifetime determinants in *Escherichia coli* cells cultured at different growth rates. *BMC Genomics*, *16*(1), 275.

Fast, A. G., & Papoutsakis, E. T. (2012). Stoichiometric and energetic analyses of non-photosynthetic CO2-fixation pathways to support synthetic biology strategies for production of fuels and chemicals. *Current Opinion in Chemical Engineering*, 380–395.

Fröstl, J., Seifritz, C., & Drake, H. L. (1996). Effect of nitrate on the autotrophic metabolism of the acetogens Clostridium thermoautotrophicum and Clostridium thermoaceticum. *Journal of Bacteriology*, *178*(15), 4597–4603.

Hasan, S. M., & Hall, J. B. (1975). The physiological function of nitrate reduction in *Clostridium perfringens*. *Journal of General Microbiology*, *87* (1975), 120–128.

Hoffmeister, S., Gerdom, M., Bengelsdorf, F. R., Linder, S., Flüchter, S., Öztürk, H., & Dürre, P. (2016). Acetone production with metabolically engineered strains of Acetobacterium woodii. *Metabolic Engineering*, *36*, 37–47.

Hu, P., Chakraborty, S., Kumar, A., Woolston, B. M., Liu, H., Emerson, D., & Stephanopoulos, G. (2016). Integrated bioprocess for conversion of gaseous substrates to liquids. *Proceedings of the National Academy of Sciences of the United States*, *113*(14), 3773–3778.

Imkamp, F., Biegel, E., Jayamani, E., Buckel, W., & Müller, V. (2007). Dissection of the caffeate respiratory chain in the acetogen Acetobacterium woodii: Identification of an Rnf-type NADH dehydrogenase as a potential coupling site. *Journal of Bacteriology*, *189*(22), 8145–8153.

Iwasaki, Y., Kita, A., Yoshida, K., Tajima, T., Yano, S., Shou, T., & Nakashimada, Y. (2017). Homolactic acid fermentation by the genetically engineered thermophilic homoacetogen *Moorella thermoacetica* ATCC 39073. *Appl. Environ. Microbiol*, *83*(8), 1–13.

Jones, S. W., Fast, A. G., Carlson, E. D., Wiedel, C. A., Au, J., Antoniewicz, M. R., Papoutsakis, E. T., & Tracy, B. P. (2016). CO2 fixation by anaerobic non-photosynthetic mixotrophy for improved carbon conversion. *Nature Communication*, *7*, 12800.

Jormakka, M., Byrne, B., & Iwata, S. (2003). Protonmotive force generation by a redox loop mechanism. *FEBS Letters*, *545*(1), 25–30.

Kersey, P. J., Allen, J. E., Armean, I., Boddu, S., Bolt, B. J., Carvalho-Silva, D., & Staines, D. M. (2016). Ensembl genomes 2016: More genomes, more complexity. *Nucleic Acids Research*, *44*(D1), D574–D580.

Köpke, M., Held, C., Hujer, S., Liesegang, H., Wiezer, A., Wollherr, A., & Dürre, P. (2010). Clostridium ljungdahlii represents a microbial production platform based on syngas. *Proceedings of the National Academy of Sciences of the United States*, *107*(34), 15305–15305.

Kracke, F., Virdis, B., Bernhardt, P. V., Rabaey, K., & Krömer, J. O. (2016). Redox dependent metabolic shift in Clostridium autoethanogenum by extracellular electron supply. *Biotechnology Biofuels*, *9*(1), 249.

Love, M. I., Huber, W., & Anders, S. (2014). Moderated estimation of fold change and dispersion for RNA-seq data with DESeq2. *Genome Biology*, *15*(12), 550.

Maier, T., Schmidt, A., Güell, M., Kühner, S., Gavin, A. C., Aebersold, R., & Serrano, L. (2011). Quantification of mRNA and protein and integration with protein turnover in a bacterium. *Molecular Systems Biology*, *7*(511), 1–12.

Millard, P., Letisse, F., Sokol, S., & Portais, J. C. (2012). IsoCor: Correcting MS data in isotope labeling experiments. *Bioinformatics*, *28*(9), 1294–1296.

Mock, J., Zheng, Y., Mueller, A. P., Ly, S., Tran, L., Segovia, S., & Thauer, R. K. (2015). Energy conservation associated with ethanol formation from H2 and CO2 in Clostridium autoethanogenum involving electron bifurcation. *Journal of Bacteriology*, *197*(18), 2965–2980.

Molitor, B., Marcellin, E., & Angenent, L. T. (2017). Overcoming the energetic limitations of syngas fermentation. *Current Opinion in Chemical Biology*, *41*, 84–92.

Moran, M. A., Satinsky, B., Gifford, S. M., Luo, H., Rivers, A., Chan, L. K., & Hopkinson, B. M. (2013). Sizing up metatranscriptomics. *ISME Journal*, *7*(2), 237–243.

Moreno-Vivián, C. (1999). Prokaryotic nitrate reduction: Molecular properties and functional distinction among bacterial nitrate reductases. *Journal of Bacteriology*, *181*(21

Nagarajan, H., Sahin, M., Nogales, J., Latif, H., Lovley, D. R., Ebrahim, A., & Zengler, K. (2013). Characterizing acetogenic metabolism using a genome-scale metabolic reconstruction of *Clostridium ljungdahlii*. *Microbial Cell Factories*, *12*, 118.

Ou, X., Zhang, X., Zhang, Q., & Zhang, X. (2013). Life-cycle analysis of energy use and greenhouse gas emissions of gas-to-liquid fuel pathway from steel mill off-gas in China by the LanzaTech process. *Frontiers in Energy*, *7*(3), 263–270.

Pedersen, S., Reeh, S., & Friesen, J. D. (1978). Functional mRNA half lives in *E. coli*. *Molecular Genetics and Genomics*, *166*(3), 329–336.

Peters, R., Hellenbrand, J., Mengerink, Y., & Van Der Wal, S. (2004). Online determination of carboxylic acids, aldehydes and ketones by high-performance liquid chromatography-diode array detection-atmospheric pressure chemical ionisation mass spectrometry after derivatization with 2-nitrophenylhydrazine. *Journal of Chromatography A*, *1031*(1-2), 35–50.

Pierce, E., Xie, G., Barabote, R. D., Saunders, E., Han, C. S., Detter, J. C., & Ragsdale, S. W. (2008). The complete genome sequence of Moorella thermoacetica (f. *Clostridium thermoaceticum*). *Environmental Microbiology*, *10*(10), 2550–2573.

Sakai, S., Nakashimada, Y., Inokuma, K., Kita, M., Okada, H., & Nishio, N. (2005). Acetate and ethanol production from H2 and CO2 by Moorella sp. using a repeated batch culture. *Journal of Bioscience and Bioengineering*, *99*(3), 252–8.

Schauer, N. L., & Ferry, J. G. (1982). Properties of formate dehydrogenase in *Methanobacterium formicicum*. *Journal of Bacteriology*, *150*(1), 1–7.

Schuchmann, K., & Müller, V. (2014). Autotrophy at the thermodynamic limit of life: A model for energy conservation in acetogenic bacteria. *Nature Reviews Microbiology*, *12*(12), 809–821.

Schüte, H., Flossdorf, J., Sahm, H., & Kula, M. R. (1976). Purification and properties of formaldehyde dehydrogenase and formate dehydrogenase from *Candida boidinii*. *European Journal of Biochemistry*, *62*, 151–160.

Seifritz, C., Daniel, S., Gossner, A., & Drake, H. (1993). Nitrate as a preferred electron sink for the acetogen Clostridium thermoaceticum. *Journal of Bacteriology*, *175*, 8008–8013.

Seifritz, C., Fröstl, J. M., Drake, H. L., & Daniel, S. L. (2002). Influence of nitrate on oxalate- and glyoxylate-dependent growth and acetogenesis by *Moorella thermoacetica*. *Archives of Microbiology*, *178*(6), 457–64.

Strickland, J., & Parsons, T. R. (1972). *A practical handbook of seawater analysis* (2nd., 167). *Ottawa,Canada: Fisheries Research Board of Canada*

Tan, Y., Liu, J., Chen, X., Zheng, H., & Li, F. (2013). RNA-seq-based comparative transcriptome analysis of the syngas-utilizing bacterium *Clostridium ljungdahlii* DSM 13528 grown autotrophically and heterotrophically. *Molecular BioSystems*, *9*(11), 2775–2784.

Thauer, R. K., Jungermann, K., & Decker, K. (1977). Energy conservation in chemotrophic anaerobic bacteria. *Bacteriology Reviews*, *41*(1), 100–180.

Tracy, B. P., Jones, S. W., Fast, A. G., Indurthi, D. C., & Papoutsakis, E. T. (2012). Clostridia: The importance of their exceptional substrate and metabolite diversity for biofuel and biorefinery applications. *Current Opinion in Biotechnology*, *23*(3), 364–81.

Tremblay, P.-L., Zhang, T., Dar, S. A., Leang, C., & Lovley, D. R. (2013). The Rnf complex of Clostridium ljungdahlii is a proton-translocating ferredoxin:NAD+ oxidoreductase essential for autotrophic growth. *MBio*, *4*(1), e00406–e00412.

Tschech, A., & Pfennig, N. (1984). Growth yield increase linked to caffeate reduction in *Acetobacterium woodii*. *Archives of Microbiology*, *137*(2), 163–167.

Ueki, T., Nevin, K. P., Woodard, T. L., & Lovley, D. R. (2014). Converting carbon dioxide to butyrate with an engineered strain of *Clostridium ljungdahlii*. *MBio*, *5*(5), 19–23.

Valgepea, K., de Souza Pinto Lemgruber, R., Meaghan, K., Palfreyman, R. W., Abdalla, T., Heijstra, B.D., & Marcellin, E. (2017). Maintenance of ATP homeostasis triggers metabolic shifts in gas-fermenting acetogens. *Cell System*, *4*, 505–515.

Valgepea, K., Loi, K., Behrendorff, J. B., Lemgruber, R. D.S., Plan, M., Hodson, M. P., & Marcellin, E. (2017). Arginine deiminase pathway provides ATP and boosts growth of the gas-fermenting acetogen Clostridium autoethanogenum. *Metabolic Engineering*, *41*, 202–211.

SUPPORTING INFORMATION

Additional supporting information may be found online in the Supporting Information section at the end of the article.

How to cite this article: Emerson DF, Woolston BM, Liu N, Donnelly M, Currie DH, Stephanopoulos G. Enhancing hydrogen-dependent growth of and carbon dioxide fixation by *Clostridium ljungdahlii* through nitrate supplementation. *Biotechnology and Bioengineering*. 2019;116:294–306. https://doi.org/10.1002/bit.26847